(Received 1 August 2023, Accepted 3 November 2023, Scheduled 13 November 2023)

Optimizing Detection in MIMO OFDM Radar: Methods for Eliminating Distance-Angle Coupling in Beamforming

Doudou Huang[1], Yurong Wu[1], Mingliang Shen[2], Longshan Xu[1,*], and Jun Tang[2,*]

[1]Department of Materials Science and Engineering, Xiamen University of Technology, Xiamen 361024, China
[2]Department of Opto-Electronic and Communication Engineering, Xiamen University of Technology, Xiamen 361024, China

ABSTRACT: This study investigates beamforming and optimization in Multiple-Input-Multiple-Output Orthogonal-Frequency-Division-Multiplexing (MIMO OFDM) radar systems. The objective of this research is to mitigate the range-angle coupling effect in MIMO OFDM radar systems by adopting range compensation and distance-angle decoupling methods, which is to ensure that the signal processing during radar waveform formation does not impact the aforementioned coupling effect. In distance compensation, the CVX toolbox is used to minimize peak sidelobe. A mathematical model is established, and an optimal set of transmission frequencies is achieved through the use of the Alternating-Direction-Method-of-Multipliers (ADMM) algorithm in the context of distance-angle decoupling. Both methods effectively eliminate distance-angle coupling and enhance detection and identification capabilities of MIMO OFDM radar systems.

1. INTRODUCTION

In recent years, the field of MIMO OFDM radar has attracted considerable interest and research focus [1–3]. This cutting-edge technology has the potential to revolutionize radar systems and find diverse applications in various domains. Despite the progress made so far, the design of appropriate MIMO OFDM radar waveforms and beams remains a challenging task [4, 5]. This is primarily due to the complex interplay of multiple parameters that need to be carefully balanced for optimal performance.

In current context, MIMO radar beamforming optimization methods can be categorized into two main approaches. The first approach involves optimizing the covariance matrix of transmitted beams under certain constraints to select suitable beamforming patterns for practical engineering projects. This theory is then used to design radiation beam patterns for individual transmitting antenna elements based on the optimized covariance matrix [6–8]. The second approach directly focuses on optimizing the actual waveforms of each transmitting antenna array element to select suitable transmitting beamforming patterns that meet practical engineering requirements [9–11].

In 2006, Antonik and others [12] proposed a distance-related beam direction diagram in the context of frequency diversity array radar. In the same year, Antonik et al. presented various waveform analyses for different transmitting modes [13] and distance-dependent array-level waveform diversity [14]. Subsequently, Secmen et al. [15] analyzed the periodicity of frequency-controlled arrays in both distance and angle dimensions. It was demonstrated in [16] that frequency-controlled array antennas exhibit periodicity in beam scanning, and reference [17] validated this periodicity using four microstrip antennas and four frequency synthesizers. Sammartino et al. [18] combined MIMO radar systems and proposed a new beam design method dependent on distance and angle. In the frequency control array radar, Sammartino et al. [19] integrated the centralized MIMO with waveform diversity and studied the beam pattern distributed MIMO with spatial diversity of frequency controlled arrays as well as the beam pattern related to distance but angle independent, providing greater flexibility. Wang and Shao [20] and Khan and Qureshi [21] proposed a time-dependent frequency offset method for frequency controlled arrays to design radar beams, which decoupled the radar beam pattern on a two-dimensional plane of distance and angle to eliminate the periodicity of the beam pattern. In [22], a subarray-based frequency-controlled array radar beam design method was proposed, which jointly estimated the distance and azimuth of the target for background application, and further proposed an array beam optimization design method based on minimizing the Cramer-Rao bound [23]. In [24], from the perspective of distance-angle decoupling, the method of frequency-controlled encoding was used to redesign the carrier combination of the array and re-optimize the Cramer-Rao bound [25].

In future MIMO OFDM radar applications, techniques such as utilizing first-order even functions (as suggested in reference [26]) for channel parameter estimation and considering the wave function concept from the nonlinear Schrödinger equation (reference [27]) may improve target localization and tracking accuracy. Additionally, the study of electromagnetic wave propagation in plasma waveguides [28] can enhance our understanding of spectrum utilization to minimize interference and optimize signal transmission. Optimization algorithms from references [29–32] may be applied to waveform design in MIMO OFDM radar systems, adding practical value to future applications.

* Corresponding authors: Longshan Xu (15980840308@126.com), Jun Tang (jtang@xmut.edu.cn).

The paper presents two methods, the distance compensation method and distance-angle decoupling method, to eliminate the distance-angle coupling effect in radar systems. The distance compensation method compensates for phase delays between received signals of array elements relative to a reference element based on distance. The distance-angle decoupling method treats the distance-angle coupling as the objective function and utilizes the ADMM algorithm to minimize it, achieving echo distance-angle decoupling. Both methods effectively improve radar performance by eliminating the distance-angle coupling effect.

2. MIMO RADAR BEAMFORMING AND OPTIMIZATION

2.1. Beamforming Optimization Based on Distance Compensation Method

Assume M and N array elements for the transmitting and receiving arrays, respectively, in the form of uniform linear arrays. The signal transmitted by the m-th array element of the transmitting array, after reflecting off a far-field point target and reaching the n-th array element of the receiving array, can be expressed as:

$$x_{n,m}(t) = \sigma s_m(t) \cdot P_{n,m}(\theta_t, \theta_r) \tag{1}$$

where σ is the radar cross section. $P_{n,m}(\theta_t, \theta_r)$ is the relative phase difference between the signals arriving at the n-th element and the reference element. θ_r and θ_t represent the incident angles at the receiving end and transmitting end, respectively, which can be written as:

$$P_{n,m}(\theta_t, \theta_r) = e^{\left[-j2\pi f_m\left(\frac{R_t+R_r}{c} - \tau_{t,m}(\theta_t) - \tau_{r.n}(\theta_r)\right)\right]} \tag{2}$$

where $\tau_{t,m}(\theta_t) = \frac{(m-1)d_t \sin(\theta_t)}{c}$ and $\tau_{r,n}(\theta_r) = \frac{(n-1)d_r \sin(\theta_r)}{c}$. d_r and d_t represent the spacing between antenna elements at the receiving end and transmitting end, respectively. R_r and R_t represent the distance terms at the transmitting end and receiving end, respectively.

If it is a mono-static radar system, $\theta_t = \theta_r$, (2) can be rewritten as:

$$P_{n,m}(\theta) = e^{\left[-j2\pi\left(\frac{R_t+R_t}{\lambda_m} - \frac{(m-1)d_t \sin(\theta)}{\lambda_m} - \frac{(n-1)d_r \sin(\theta)}{\lambda_m}\right)\right]} \tag{3}$$

The distance terms $\frac{R_t+R_r}{\lambda_m}$ of multi-carrier signals introduce varying phase differences for transmission signals of different frequencies when they arrive at the same receiving array element. Therefore, distance compensation is applied during angle-domain beamforming [33, 34]. After compensation, Equation (3) can be rewritten as:

$$P_{n,m}(\theta) = e^{\left[j2\pi\left(\frac{(m-1)d_t \sin(\theta)}{\lambda_m} + \frac{(n-1)d_r \sin(\theta)}{\lambda_m}\right)\right]} \tag{4}$$

In an ideal scenario, all signal transmission and reception channels exhibit identical responses, and the total received signal by the receiving array is denoted as:

$$x(t) = \sum_{n=1}^{N}\sum_{m=1}^{M} x_{n,m}(t) \tag{5}$$

Express the above Equation (5) in vector form:

$$\mathrm{X}(t) = \alpha(\theta_t, \mathbf{F}) \cdot \beta^{\mathbf{H}}(\theta_r) \cdot \sigma s(t) \tag{6}$$

where $\alpha(\theta_t, \mathbf{F}) = \left[1, e^{\left(\frac{j2\pi d_t \sin(\theta)}{\lambda_2}\right)}, \cdots, e^{\left(\frac{j2\pi(M-1)d_r \sin(\theta)}{\lambda_M}\right)}\right] \in \mathbf{C}^{M\times 1}$ and

$$\beta(\theta_r) = \left[1, e^{\left(\frac{j2\pi d_r \sin(\theta)}{\lambda_2}\right)}, \cdots, e^{\left(\frac{j2\pi(M-1)d_t \sin(\theta)}{\lambda_N}\right)}\right] \in \mathbf{C}^{N\times 1}$$

is the steering vector of the transmitted signals from each array element and the receiving channel, respectively. $\mathbf{F} = (f_0, f_1, \cdots, f_M)$ represents the frequencies of the transmitted signals at each array element.

The element λ in $\beta(\theta_r)$ is a variable whose value is the same as the λ in the first term of the summation in equation (4). This is because the first term of the summation in Equation (4) is a component of $\alpha(\theta_t, \mathbf{F})$, while the second term is a component of $\beta(\theta_r)$. Equation (4) effectively extends the vector representation of the single-carrier array signal model to the result of the multi-carrier orthogonal waveform MIMO radar. The second term in Equation (4) reflects the diversity characteristic of orthogonal waveform MIMO radar waveforms. In the first term of equation (4), m takes on any value from 1 to any one of M, and in the second term of Equation (4), n ranges from 1 to N, equivalent to the Kronecker product of the transmitting steering vector and receiving steering vector. When m ranges from 1 to M, a vector of size $N \times M$ rows and 1 column is obtained. The physical interpretation of m taking values from 1 to M is the transmission of signals on multiple carrier frequencies. Thus, the transmitting-receiving joint steering vector pointing to the direction of θ is represented as:

$$Ar(\theta_r) = \beta_1(\theta) \otimes \beta_2(\theta) \otimes \cdots \otimes \beta_N(\theta) \tag{7}$$

To optimize the total sidelobe energy, the objective function is expressed as:

$$\max_{\theta} J(\theta) = \frac{1}{N}\sum_{i=1}^{N} |s_i(\theta)|^2 \tag{8}$$

where $s_i(\theta) = e^{\frac{-j2\pi(N-1)d\sin(\theta)}{\lambda_i}}$ represents the received signal, and i denotes the i-th antenna.

The total sidelobe energy can be calculated using the formula:

$$P_{side}(\theta) = \frac{1}{N}\sum_{i=1}^{N}\left|\sum_{j\neq i} k_j(\theta) x_j\right|^2 \tag{9}$$

where x_i represents the i-th transmitted signal and $|x_i|^2$ represents the power of the i-th transmit signal.

The objective function is reformulated as:

$$\max_{\omega} J(\omega) = \frac{E\left[|y(\theta)|^2\right]}{E\left[|d(\theta)|^2\right]} \tag{10}$$

where E denotes the expectation operation, $y(\theta)$ the beamforming output, $d(\theta)$ the desired signal, and the physical meaning of this objective function is to maximize the energy of the beamforming output while minimizing the energy of the sidelobes.

In the same radar system, the required signal energy is usually constant, so the objective function can be simplified to $\max y(\theta)$.

To maximize signal power, the beamforming weight vector is obtained by projecting the transmitting-receiving joint steering vector onto it, resulting in the output signal: $y(\theta) = \omega^H Ar(\theta_{SL}) + n$. Constraint $\omega^H Ar_0(\theta_0) = 1$ is applied to convert MIMO OFDM radar beamforming into a constraint optimization problem, aiming to find optimal weights with minimized sidelobes. The mathematical representation of the objective function with constraints is as follows:

$$\min_{\omega} \max_{\theta_{SL}\in\Theta_{SL}} \left|\omega^H Ar\left(\theta_{SL}\right)\right|$$

$$s.t.\omega^H Ar_0\left(\theta_0\right) = 1 \tag{11}$$

where θ_{SL} includes all angles within the sidelobe range, and θ_0 represents the azimuth angle of the reference target.

This problem is a constrained convex optimization task involving an objective function. The optimal weight vector is determined using the CVX toolbox [35], and then it is used in equation (10) to create the optimized beam pattern.

2.2. Beamforming Optimization Based on Distance-angle Decoupling Method

In the assumed scenario, considering a target with a length of L meters and a scanning angle φ between the target and the radar line of sight, the requirement for the cross-correlation of target echoes received by adjacent array elements imposes a relationship on the frequency increment between adjacent elements: $\Delta f = \frac{c}{2L\sin(\varphi)}$. This relationship allows the calculation of the frequency increment between adjacent array elements. For the MIMO OFDM radar system discussed in this paper, which employs a uniform linear array for multi-frequency MIMO radar, there exists coupling between distance and elevation angle. The signal model established is as follows:

The elevation measurement error caused by distance measurement inaccuracies and the distance measurement error resulting from elevation measurement inaccuracies are expressed as follows:

$$\varepsilon_{\Delta\theta}\left(\Delta R\right) = \frac{\sum_{k=1}^{N} w_k\beta_{ek}}{\sum_{k=1}^{N}\beta_{ek}^2 + \sum_{l=1}^{N}\beta_{rl}^2}\Delta R$$

$$\varepsilon_{\Delta R}\left(\Delta\theta\right) = \frac{\sum_{k=1}^{N} \alpha_{ek}\beta_{ek}}{\sum_{k=1}^{N}\beta_{ek}^2 + \sum_{l=1}^{N}\beta_{rl}^2}\Delta\theta \tag{12}$$

where k is the k-th array element, θ the elevation angle, ΔR the range quantization error, and $\Delta\theta$ the elevation angle measurement error.

$$w_k = \frac{4\pi\left(f_k - f_0\right)}{c}$$

$$\beta_{ek} = \frac{2\pi f_k d\sin\left(\theta\right)}{c} \tag{13}$$

where f_k is the frequency of the k-th array element. Therefore, the numerator terms for elevation and range measurement errors can be rewritten as:

$$\sum_{k=1}^{N} w_k\beta_{ek} = \frac{4kf_k\sin\left(\theta\right)\pi^2}{c}\left(\frac{f_k}{f_0} - 1\right) \tag{14}$$

To minimize the impact of range-elevation coupling, the objective function can be established as follows:

$$\min\left\{\left|\varepsilon_{\Delta\theta}\left(\Delta R\right)\right| + \left|\varepsilon_{\Delta R}\left(\Delta\theta\right)\right|\right\} \tag{15}$$

Ultimately, the range-elevation coupling problem has been transformed into a mathematical optimization problem with constraints, and the mathematical model is as follows:

$$\min\left|\frac{4kf_k\sin\left(\theta\right)\pi^2}{c}\left(\frac{f_k}{f_0} - 1\right)\right|$$

$$\text{s.t. } f_{k,\min} \le f_k \le f_{k,\max} \tag{16}$$

The objective function exhibits convexity [36], allowing the use of the ADMM algorithm [37]. By incorporating constraints, the augmented Lagrangian function is obtained as follows:

$$L\left(y, f_k, u, z\right) = \sum_{k=1}^{K} u_k\left(y - \frac{4kf_k\sin\left(\theta\right)\pi^2}{c}\left(\frac{f_k}{f_0} - 1\right) - z_k\right)$$

$$+\frac{\rho}{2}\sum_{k=1}^{K}\left(y - \frac{4kf_k\sin\left(\theta\right)\pi^2}{c}\left(\frac{f_k}{f_0} - 1\right) - z_k\right)^2 + y \tag{17}$$

where $y = \left|\frac{4kf_k\sin(\theta)\pi^2}{c}\left(\frac{f_k}{f_0} - 1\right)\right|$, u is the Lagrange multiplier, and it is a scalar. z is the auxiliary variable. ρ is a positive penalty parameter.

Then, alternating updates of y, f_k, z, and u:

(1) Update y:

$$y^{t+1} = \arg\min y\, L\left(y, f_k^t, u^t, z^t\right) \tag{18}$$

By solving the derivative of this equation to be 0, we can obtain the analytical solution of y^{t+1}:

$$y^{t+1} = \frac{\sum_{k=1}^{K}\left(4kf_k^2\frac{\sin(\theta)\pi^2}{c}\left(\frac{f_k}{f_0} - 1\right) + \rho z^t - u^t\right)}{\sum_{k=1}^{K} 4k^2 f_k^2\frac{\sin(\theta)\pi^2}{c} + \rho} \tag{19}$$

(2) Update f_k:

$$f_k{}^{t+1} = \arg\min\ f_k L\left(y^{t+1}, f_k, u^t, z^t\right) \tag{20}$$

By solving the derivative of this equation to be 0, we can obtain the analytical solution of f_k^{t+1}:

$$f_k^{t+1} = \frac{\frac{\sqrt{\rho}\sqrt{\left(\frac{4k^2\sin(\theta)\pi^2}{c}+\rho\right)}}{8k\sin(\theta)\frac{\pi^2}{c}} - \frac{1}{2f_0}}{1+\frac{c^2\rho}{8k^2\sin^2(\theta)\pi^4}} \tag{21}$$

(3) Update z:

$$z_k^{t+1} = \max\left(0, y^{t+1} + 4kf_k^{t+1}\frac{\sin(\theta)\pi^2}{c}\left(\frac{f_k^{t+1}}{f_0}-1\right)+u_k^t\right) \tag{22}$$

(4) Update u:

$$u_k^{t+1} = u_k^t + y^{t+1} - 4kf_k^{t+1}\frac{\sin(\theta)\pi^2}{c}\left(\frac{f_k^{t+1}}{f_0}-1\right) - z_k^{t+1} \tag{23}$$

(5) Determining the convergence criterion for termination of iterations:

$$\left|y^t - y^{t-1}\right| < \varepsilon \tag{24}$$

where ε is the required precision for the convergence criterion.

Repeating alternate updates of y, f_k, z, and u until convergence. When the iteration reaches convergence, that is, satisfies the stopping criterion, and the final output Equation (16) achieves the minimum value, the value of each f_k is obtained.

The principle of correlating echoes between elements of the MIMO OFDM radar transmitting array allows computation of

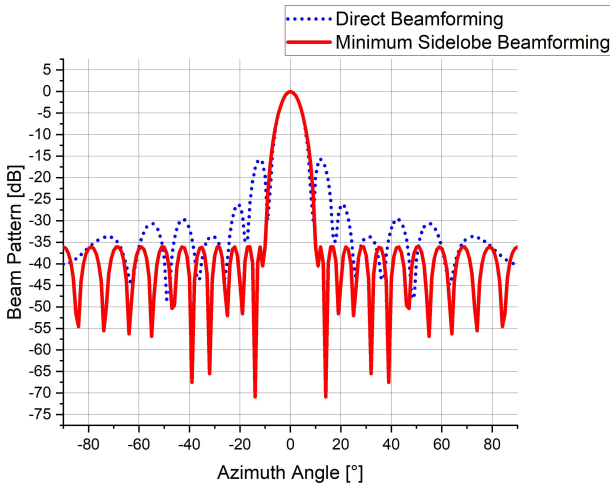

FIGURE 1. Distance compensation method: Conventional beamforming vs. Beamforming with optimize weight vector, $d_t = d_r$.

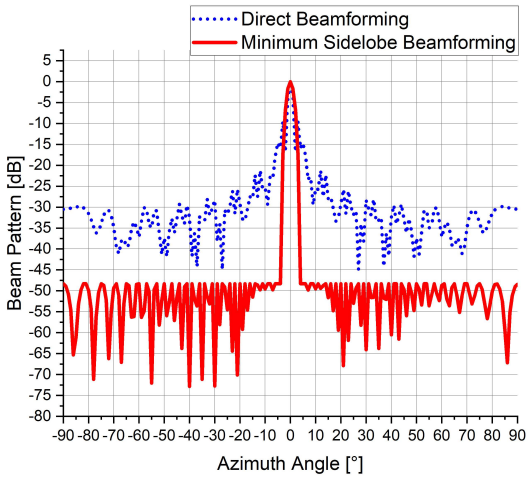

FIGURE 2. Distance compensation method: Conventional beamforming vs. Beamforming with optimize weight vector, $d_t = Nd_r$.

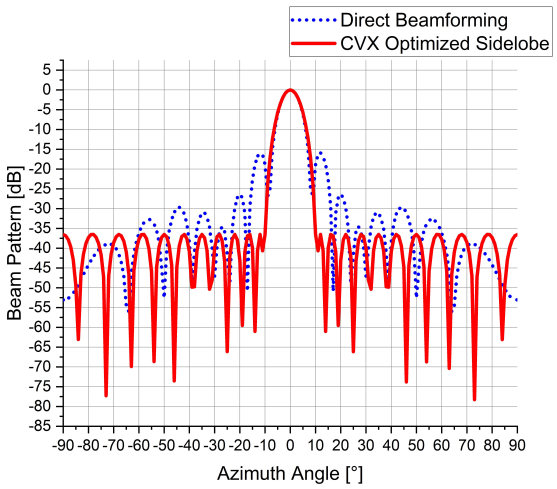

FIGURE 3. Distance-Angle decoupling method: Conventional beamforming vs. Beamforming with optimize weight vector, $d_t = d_r$.

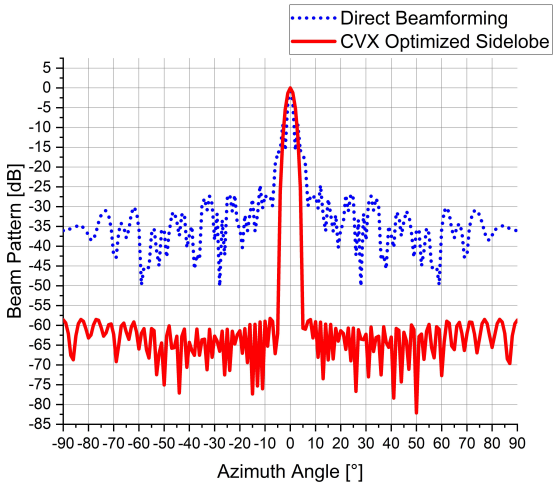

FIGURE 4. Distance-Angle decoupling method: Conventional beamforming vs. Beamforming with optimize weight vector, $d_t = Nd_r$.

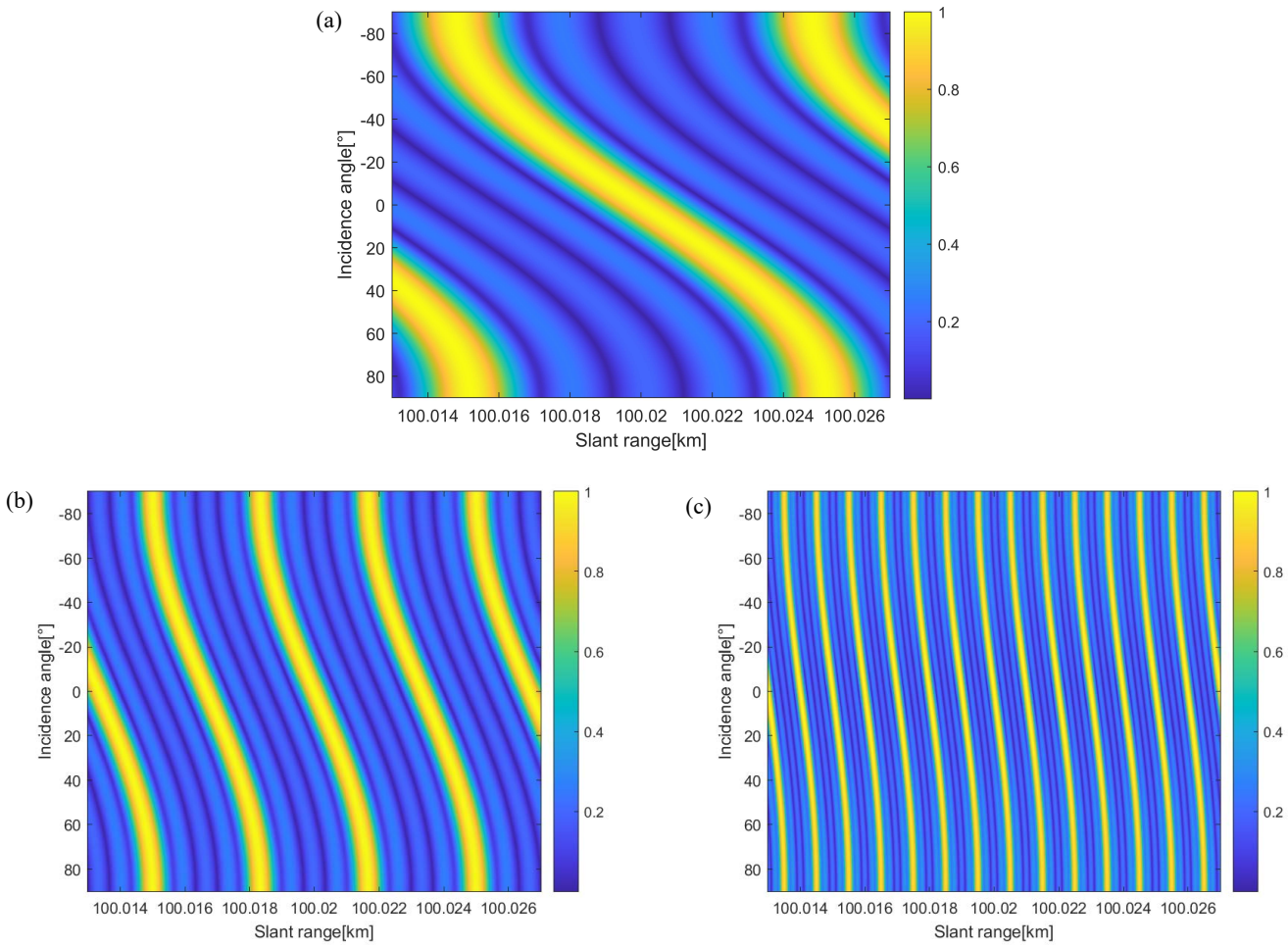

FIGURE 5. Projection of unoptimized radar beamforming 3D plot with default frequencies. (a) $\Delta f_1 = 30\,\text{kHz}$. (b) $\Delta f_2 = 90\,\text{kHz}$. (c) $\Delta f_3 = 30\,\text{MHz}$.

the optimal carrier frequency combination. The coupling effect between range and angle is taken as the objective function, and it is computed using the ADMM to minimize this objective function. The resulting optimal carrier frequency combination is then utilized as the frequency combination for the transmitting array, aiming to achieve the decoupling of echo in terms of range and angle. The choice of the ADMM algorithm is motivated by its suitability for convex optimization problems. For convex optimization problems, the ADMM algorithm guarantees convergence to the global optimum, thus avoiding the complexities associated with matrix operations and optimization. This approach reduces computational complexity and enhances target detection performance.

3. NUMERICAL RESULTS BETWEEN THE DISTANCE COMPENSATION METHOD AND THE DISTANCE-ANGLE DECOUPLING METHOD

The objective of this section is to simulate MIMO OFDM radar angle-dimensional beamforming by utilizing the signal model and objective functions established earlier, along with the specification of relevant simulation parameters. The feasibility of the proposed radar beamforming optimization technique is verified through numerical results.

We begin by considering a transmitting array with $M = 5$ elements and a receiving array with $N = 13$ elements. The reference element's carrier frequency is set to $f_0 = 30\,\text{GHz}$, and the corresponding wavelength is $\lambda = c/f_0$, where c is the speed of light. The inter-element spacing is set to $d = \lambda/4$. The carrier frequencies of the transmit array elements linearly increase starting from the reference element, with the m-th element's carrier frequency denoted as $f_m = f_0 + (m-1)\Delta f$ [38], where Δf represents the frequency increment.

The target distance is set to $L = 10$ meters, the radar's scanning angle fixed at $\varphi = 30°$, and the elevation angle θ set to $60°$. To compare the results between different methods, the number of transmitting elements is set to $K = 5$. The angles in the sidelobe region are within the range $[-90° : -10, 10 : 90°]$, and the target azimuth angle θ_0 is $0°$. The constraint range for frequency is limited to $\left[2.71 \times 10^9, 3.31 \times 10^9\right]$ to avoid interference and achieve high resolution. The convergence criterion is set to $\varepsilon = 10^{-6}$.

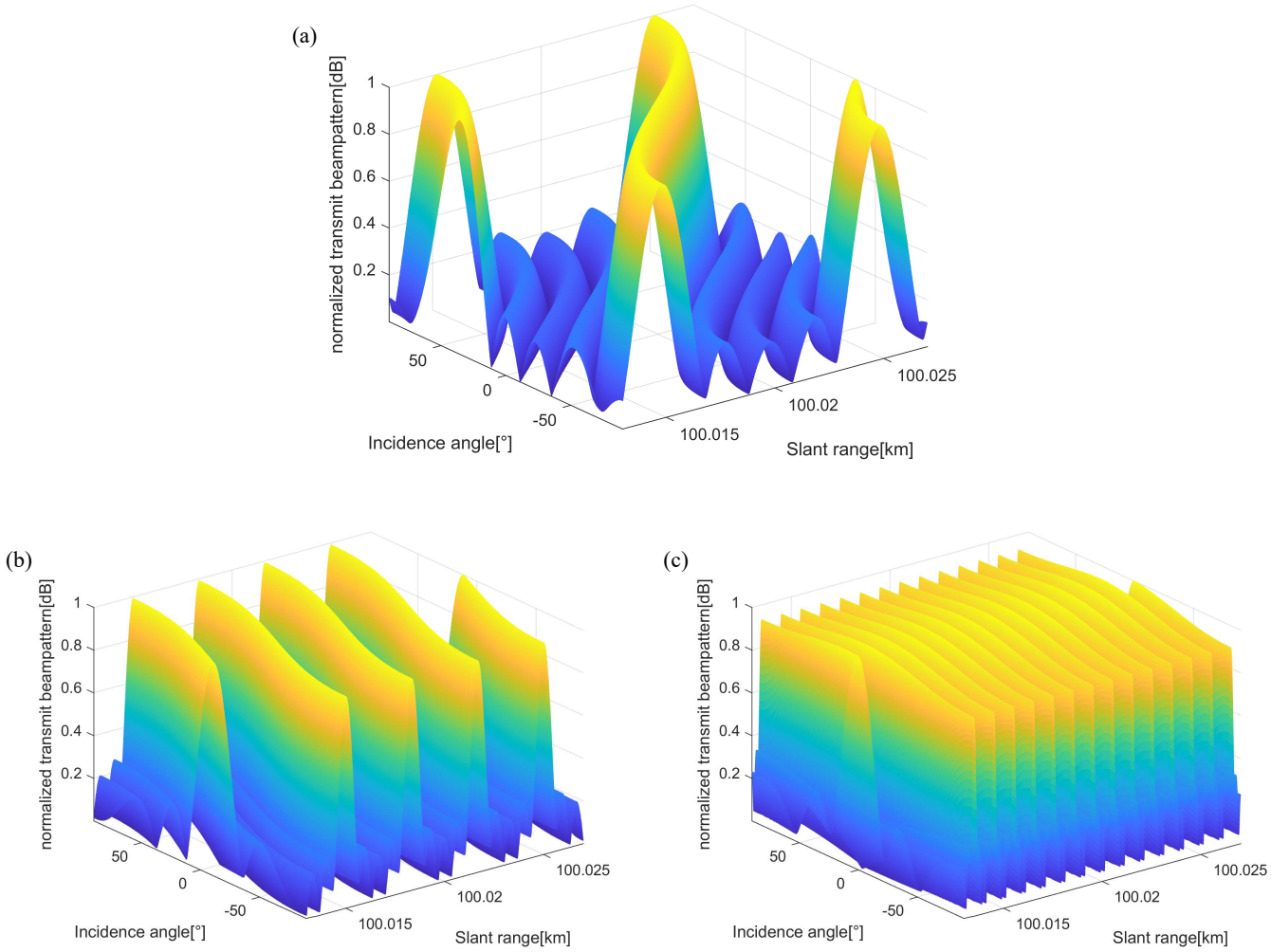

FIGURE 6. Projection of unoptimized radar beamforming 3D plot with default frequencies. (a) $\Delta f_1 = 30\,\text{kHz}$. (b) $\Delta f_2 = 90\,\text{kHz}$. (c) $\Delta f_3 = 30\,\text{MHz}$.

3.1. Distance Compensation Method

In this study, a simulation analysis was conducted to examine MIMO OFDM radar beamforming based on the proposed signal model. The unoptimized and optimized radar beam patterns were compared in Fig. 1 and Fig. 2, respectively, for cases where $d_t = d_r$ and $d_t = Nd_r$ in the radar's angular dimension. The initial carrier frequency is $f_0 = 30\,\text{GHz}$ with a frequency spacing of $\Delta f = 30\,\text{MHz}$, resulting in additional carrier frequency components: $f_1 = 3.03\,\text{GHz}$, $f_2 = 3.06\,\text{GHz}$, $f_3 = 3.09\,\text{GHz}$, and $f_4 = 3.12\,\text{GHz}$, corresponding to $M = 5$ components.

The unoptimized radar beam pattern exhibits sidelobes only 15 dB lower than the main lobe, indicating potential interference with the radar system requirements. In order to address this issue, with the objective of minimizing sidelobe levels, beamforming is achieved by adjusting weight vectors. Since the optimization problem is convex in nature, it is solved using the CVX toolbox. By optimizing the weight vectors, the main lobe of the beamforming becomes more focused, and the sidelobes are reduced, thereby achieving a lower peak sidelobe level. The optimized beam patterns in Fig. 1 and Fig. 2 showed increased main lobe widths after optimization, from $18°$ to $22°$ and from $4°$ to $8°$, respectively. This wider coverage of the main lobe effectively distributed the energy over a broader angular range.

Moreover, the optimization process significantly reduced the sidelobe levels. In Fig. 1, the sidelobe level decreased from $-15.7396\,\text{dB}$ (unoptimized) to $-36.0532\,\text{dB}$ (optimized), and in Fig. 2, it decreased from $-9.51587\,\text{dB}$ (unoptimized) to $-48.3097\,\text{dB}$ (optimized).

The optimization successfully mitigated distance-angle coupling effects, resulting in reduced sidelobes and concentrated main lobes, leading to a substantial enhancement in beamforming suppression performance.

3.2. Distance-Angle decoupling method

Table 1 presents the objective function with minimal distance-angle coupling effects, and the optimal frequency combination for transmitting signals is obtained using the ADMM algorithm.

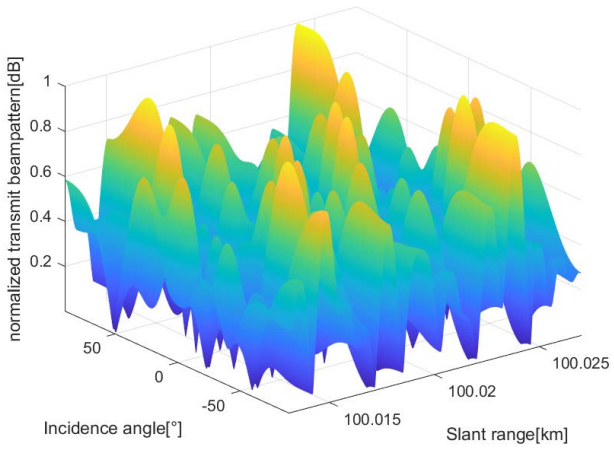

FIGURE 7. Projection of radar beamforming 3D plot optimized by ADMM algorithm.

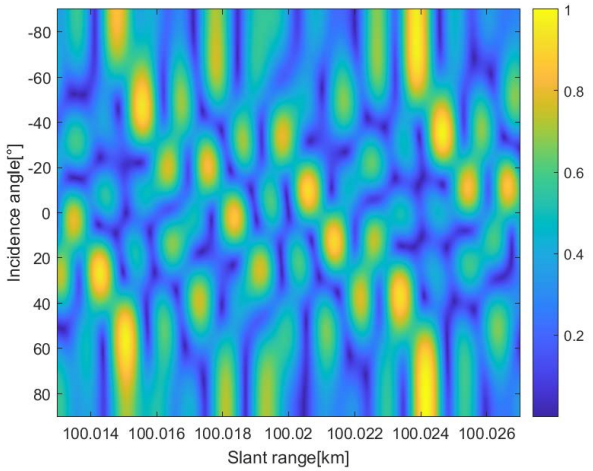

FIGURE 8. Radar beamforming 3D plot optimized by ADMM algorithm.

TABLE 1. ADMM algorithm optimization of combined carrier signals

No. (Carrier)	Hz
Carrier Frequency 1	2865510460
Carrier Frequency 2	3000026569
Carrier Frequency 3	3066660112
Carrier Frequency 4	3105583367
Carrier Frequency 5	2808905056

Figs. 3 and 4 show the radar's angular dimension beam patterns for $d_t = d_r$ and $d_t = Nd_r$, respectively. Further optimization using the CVX toolbox yields the optimized radar beam patterns. In Fig. 3, sidelobe levels are noticeably reduced after optimization, from -15.9147 dB to -40.6656 dB. Within the sidelobe region of $[-90° : -10°, 10° : 90°]$, the lowest sidelobe value reaches -78.279 dB. Similarly, in Fig. 4, the sidelobe level significantly decreases from the unoptimized value of -9.31982 dB to -58.2488 dB. Within the sidelobe region of $[-90° : -5°, 5° : 90°]$, the lowest sidelobe value reaches -82.1211 dB.

In addition, a comparison of 3D radar beam patterns and their projections can be observed between Figs. 5 and 6. We investigated the impact of interelement frequency increments on distance-angle coupling without decoupling distance and angle. The selected frequency increments were $\Delta f_1 = 30$ kHz, $\Delta f_2 = 90$ kHz, and $\Delta f_3 = 30$ MHz.

When the frequency increment was 30 kHz (Fig. 5(a)), the maximum value occurred at approximately 10 meters. For 90 kHz (Fig. 5(b)), it was at approximately 4 meters, and for 30 MHz (Fig. 5(c)), even shorter. Increasing the frequency increment reduced the maximum value distance period of the beam pattern, improving detection speed and efficiency, but compromising accuracy and resolution due to the narrower detection range, especially for distant targets.

Achieving a shorter maximum value distance period required significantly increasing the radar system's frequency increment, leading to increased complexity. At higher frequency increments, beamforming optimization did not yield desirable results. Thus, we chose $\Delta f_1 = 30$ kHz as the appropriate frequency increment.

Then, Figs. 5 and 6 reveal that the unoptimized initial carrier frequency combination exhibits interdependencies rather than independent amplitude values at various distances and angles. Multiple peaks exist in the angular dimension, forming an elliptical-shaped beam pattern, indicating the presence of distance-angle coupling effects throughout the entire angular dimension. In contrast, in Figs. 7 and 8, after optimizing the transmission carrier frequency combination, the beam pattern exhibits only a single main lobe in the angular dimension, without multiple peaks. The optimized radar beam pattern shows a more concentrated main lobe, lower sidelobes, and fewer bright spots, forming a circular transmission beam pattern, effectively eliminating the distance-angle coupling effects. Moreover, the optimized frequency differences between adjacent array elements for signal transmission are all greater than 30 MHz and are no longer equal. This optimization of frequency differences effectively controls the phase of the transmitted signal, thereby controlling the directionality of the radar transmission beam, enabling precise targeting of desired targets and enhancing the performance and efficiency of the radar system.

4. CONCLUSION

This paper presents a novel approach to address the challenge of reconciling slow-time and fast-time signal processing in MIMO OFDM radar beamforming. The key innovation lies in the introduction of frequency diversity to the transmitting array. In radar systems, frequency diversity is the technique of decomposing a radar signal into multiple subcarriers, each with a different frequency. This decomposition is achieved through OFDM technology, which divides a high-speed data stream into several low-speed data streams. Each low-speed data stream is modulated onto different subcarriers, and the orthogonality

between these subcarriers helps mitigate frequency-domain interference. However, there exists a trade-off between fast-time and slow-time processing. By applying the optimal carrier frequency increment to the transmitting array elements, the cross-correlation among echoes received by different array elements can be minimized, thereby improving target detection performance in the slow-time domain. This represents an enhancement stemming from slow-time signal processing.

Nonetheless, within the entire array pulse echo, there is coupling between range and angle, which is detrimental to fast-time signal processing. This paper, taking into account the physical reality, employs the Alternating Direction Method of Multipliers (ADMM) algorithm to optimize the transmitting carrier frequency combination for array elements. This optimization ensures both the decorrelation of echoes among array elements and the decoupling of range and angle within the entire array pulse echo. Consequently, this approach enhances the performance of slow-time signal processing while preserving the performance of fast-time signal processing.

In summary, the methods presented in this article address the conflict between MIMO OFDM radar performances in slow-time and fast-time signal processing. They optimize beamforming, resulting in a narrower main lobe and reduced side lobes.

ACKNOWLEDGEMENT

The authors would like to express their gratitude to the anonymous reviewers for their constructive comments and valuable suggestions, which significantly improved the quality of the manuscript. Additionally, the authors extend their appreciation to Professor Jun Tang for his guidance throughout the research, as well as to Professor Longshan Xu for providing substantial support in facilitating the timely requirements of this study.This research has been supported by the National Natural Science Foundation of China (No.61801412) and the Technology Program of Fujian Province (No.2020J01298). The authors express their gratitude to the valuable feedback provided by the reviewers.

REFERENCES

[1] Cao, Y. H., X. G. Xia, and S. H. Wang, "IRCI free colocated MIMO radar based on sufficient cyclic prefix OFDM waveforms," *IEEE Transactions on Aerospace and Electronic Systems*, Vol. 51, No. 3, 2107–2120, 2015.

[2] Wu, X. H., A. A. Kishk, and A. W. Glisson, "MIMO-OFDM radar for direction estimation," *IET Radar, Sonar & Navigation*, Vol. 4, No. 1, 28–36, 2010.

[3] Bao, D., G. Qin, J. Cai, and G. Lic, "A precoding OFDM MIMO radar coexisting with a communication system," *IEEE Transactions on Aerospace and Electronic Systems*, Vol. 55, No. 4, 1854–1877, 2018.

[4] Johnston, J., L. Venturino, E. Grossi, M. Lops, and X. Wang, "MIMO OFDM dual-function radar-communication under error rate and beampattern constraints," *IEEE Journal on Selected Areas in Communications*, Vol. 40, No. 6, 1951–1964, 2022.

[5] Friedlander, B., "On transmit beamforming for MIMO radar," *IEEE Transactions on Aerospace & Electronic Systems*, Vol. 48, No. 4, 3376–3388, 2012.

[6] Stoica, P., J. Li, and Y. Xie, "On probing signal design for MIMO radar," *IEEE Transactions on Signal Processing*, Vol. 55, No. 8, 4151–4161, 2007.

[7] Ahmed, S., J. S. Thompson, Y. R. Petillot, and B. Mulgrew, "Unconstrained synthesis of covariance matrix for MIMO radar transmit beampattern," *IEEE Transactions on Signal Processing*, Vol. 50, No. 8, 3837–3849, 2011.

[8] Skolnik, M. I., *Radar Handbook*, McGraw-Hill, New York, 2008.

[9] Ahmed, S. and M. S. Alouini, "MIMO radar transmit beampattern design without synthesising the covariance matrix," *IEEE Transactions on Signal Processing*, Vol. 62, No. 9, 2278–2289, 2014.

[10] Imani, S., M. M. Nayebi, and S. A. Ghorashi, "Transmit signal design in colocated MIMO radar without covariance matrix optimization," *IEEE Transactions on Aerospace and Electronic Systems*, Vol. 53, No. 5, 2178–2186, 2017.

[11] Bouchoucha, T., S. Ahmed, T. Al-Naffouri, and M. S. Alouini, "DFT-based closed-form covariance matrix and direct waveforms design for MIMO radar to achieve desired beampatterns," *IEEE Transactions on Signal Processing*, Vol. 65, No. 8, 2104–2113, 2017.

[12] Antonik, P., M. C. Wicks, H. D. Griffiths, and C. J. Baker, "Frequency diverse array radars," *IEEE Conference on Radar*, 3, 2006.

[13] Antonik, P., M. C. Wicks, H. D. Griffiths, and C. J. Baker, "Multi-mission multi-mode waveform diversity," *IEEE Conference on Radar*, 3, 2006.

[14] Antonik, P., M. C. Wicks, H. D. Griffiths, and C. J. Baker, "Range dependent beamforming using element level waveform diversity," *International Waveform Diversity & Design Conference*, 3, 2006.

[15] Secmen, M., S. Demir, A. Hizal, and T. Eker, "Frequency diverse array antenna with periodic time modulated pattern in range and angle," *IEEE Radar Conference*, 427–430, 2007.

[16] Huang, J., et al., "Frequency diverse array with beam scanning feature," *IEEE International Antennas and Propagation Symposium*, 1, 2008, DOI: 10.1109/APS.2008.4619415).

[17] Huang, J. J., K.-F. Tong, and C. J. Baker, "Frequency diverse array: simulation and design," *IEEE Antennas and Propagation Society International Symposium*, 1–4, 2008.

[18] Sammartino, P. F., C. J. Baker, and H. D. Griffiths, "Frequency diverse MIMO techniques for radar," *IEEE Transactions on Aerospace and Electronic System*, Vol. 49, No. 1, 201–222, 2013.

[19] Sammartino, P. F., C. J. Baker, and H. D. Griffiths, "Range-angle dependent waveform," *IEEE Radar Conference*, 511–515, 2010.

[20] Wang, W. Q. and H. Shao, "Range-angle localization of targets by a double-pulse frequency diverse array radar," *IEEE Journal of Selected Topics in Signal Processing*, Vol. 8, No. 1, 106–114, 2014.

[21] Khan, W. and I. M. Qureshi, "Frequency diverse array radar with time-dependent frequency offset," *IEEE Antennas and Wireless Propagation Letters*. Vol. 13, 758–761, 2014.

[22] Wang, W. Q., "Subarray-based frequency diverse array for target range-angle estimation," *IEEE Transactions on Aerospace and Electronic Systems*, Vol. 50, No. 4, 3057–3067, 2014.

[23] Wang, Y. B., W. Q. Wang, H. Chen, and H. Z. Shao, "Optimal frequency diverse array design with Cramér-Rao lower bound minimization," *IEEE Antennas and Wireless Propagation Letters*, Vol. 14, 1188–1191, 2015.

[24] Xiong, J., W. Q. Wang, and H. Chen, "Frequency diverse array transmit beampattern optimization with genetic algorithm," *IEEE Antennas and Wireless Propagation Letters*, Vol. 16, 469–

472, 2017.

[25] Xiong, J., W. Q. Wang, and Z. Wang, "Optimization of frequency increments via CRLB minimization for frequency diverse array," *IEEE Radar Conference*, 0645–0650, 2017.

[26] Yang, X. J., A. A. Alsolami, and A. R. Ali, "An even entire function of order one is a special solution for a classical wave equation in one-dimensional space," *Thermal Science*, Vol. 27, 491–495, 2023.

[27] Islam, S., B. Halder, and A. Refaie Ali, "Optical and rogue type soliton solutions of the $(2+1)$ dimensional nonlinear Heisenberg ferromagnetic spin chains equation," *Scientific Reports*, Vol. 13, 9906, 2023.

[28] Refaie Ali, A., N. T. M. Eldabe, and A. E. H. Abd El Naby, "EM wave propagation within plasma-filled rectangular waveguide using fractional space and LFD," *The European Physical Journal Special Topics*, 1–7, 2023.

[29] Osman, M. S., K. U. Tariq, and A. Bekir, "Investigation of soliton solutions with different wave structures to the $(2+1)$-dimensional Heisenberg ferromagnetic spin chain equation," *Communications in Theoretical Physics*, Vol. 72, 035002 2020.

[30] Thota, S. and S. D. Kumar, "A new reduction algorithm for differential-algebraic systems with power series coefficients," *Information Sciences Letters*, Vol. 10, 59–66 2021.

[31] Chiroma, H., S. Abdulkareem, A. Abubakar, and A. Hermawan, "Neural networks optimization through genetic algorithm searches: A review," *Applied Mathematics & Information Sciences*, Vol. 11, 1543–1564, 2017.

[32] Mirzazadeh, M., M. Eslami, and A. H. Bhrawy, "Solitons and other solutions to complex-valued Klein-Gordon equation in ϕ-4 field theory," *Applied Mathematics & Information Sciences*, Vol. 9, 2793, 2015.

[33] Godara, L. C., "Application of antenna arrays to mobile communications. II. Beamforming and direction-of-arrival considerations," *Proceedings of the IEEE*, Vol. 85, No. 8, 1195–1245, 1997.

[34] Yang, J. R., S. Hong, and D. W. Kim, "A distance-compensated radar sensor with a six-port network for remote distinction of objects with different dielectric constants," *Journal of Electromagnetic Waves and Applications*, Vol. 24, No. 11–12, 1429–1437, 2010.

[35] Grant, M. and S. Boyd, *CVX Users' Guide*, Stanford University, Palo Alto, 2009.

[36] Boyd, S. and L. Vandenberghe, *Convex Optimization*, Cambridge University Press, New York, 2004.

[37] Hallac, D., C. Wong, S. Diamond, A. Sharang, R. Sosic, S. Boyd, and J. Leskovec, "SnapVX: A network-based convex optimization solver," *The Journal of Machine Learning Research*, Vol. 18, 1–5, 2017.

[38] Zhang, J. J. and A. Papandreou-Suppappola, "A MIMO radar with frequency diversity," *International Waveform Diversity and Design Conference*, 208–212, 2009.